arXiv:1407.1217v1 [cond-mat.quant-gas] 4 Jul 2014

Trojan quasiparticles

Bettina Gertjerenken* and Martin Holthaus
Institut für Physik, Carl von Ossietzky Universität, D-26111 Oldenburg, Germany
(Dated: July 3, 2014)

We argue that a time-periodically driven bosonic Josephson junction supports stable, quasiparticle-like collective response modes which are N-particle analogs of the nonspreading Trojan wave packets known from microwave-driven Rydberg atoms. Similar to their single-particle counterparts, these collective modes, dubbed "flotons", are well described by a Floquet-Mathieu approximation, and possess a well-defined discrete set of excitations. In contrast to other, "chaotic" modes of response, the nonheating Trojan modes conform to a mean-field description, and thus may be of particular interest for the more general question under which conditions the reduction of quantum N-particle dynamics to a strongly simplified mean-field evolution is feasible. Our reasoning is supported by phase-space portraits which reveal the degree of correspondence beween the N-particle dynamics und the mean-field picture in an intuitive manner.

PACS numbers: 03.75.Kk, 03.75.Lm, 03.65.Sq, 05.45.Mt

I. INTRODUCTION

The Trojan asteroids move around the sun close to the stable Lagrangian points L_4 and L_5 of Jupiter, sharing its orbit [1]. It was established only recently that also Earth has a co-orbiting Trojan companion, named $2010\mathrm{TK}_7$, whose orbit is stable over at least ten thousand years [2]. In a seminal paper, Bialynicki-Birula, Kaliński, and Eberly have pointed out that this classical, stable, periodic asteroid motion has a quantum analog in microwave-driven Rydberg atoms which emerges when the classical Kepler frequency of the orbiting electron equals the microwave frequency [3]; the nonspreading wave functions describing the entailing stable, though nonstationary states were aptly termed Trojan wave packets [4, 5]. In a pioneering experiment, such nondispersive Trojan wave packets could be observed with Li Rydberg atoms for more than 15 000 cycles [6]; meanwhile even Trojans with principal quantum numbers close to $n = 600$ have been generated in a controlled manner [7]. Theoretically, Trojan wave packets have been identified as Floquet states with ground state-like properties which arise upon quantization of a resonance zone in classical phase space [8–10].

Here we argue that Trojan states can also occur in quantum many-body systems, and then have to be regarded as stable quasiparticles which possess a well-defined discrete set of excitations. As a specific example, we consider a Bose-Einstein condensate in a double-well potential, *i.e.*, a "bosonic Josephson junction" [11], which is modulated periodically in time [12, 13]. When the driving frequency is resonant, such that it matches the slowly varying level spacing at a particular unperturbed state, we predict stable, nonheating, collective modes of response exhibiting properties typical of Trojan single-particle wave packets.

We proceed as follows: In Sec. II we introduce our model system and its mean-field description. In Sec. III we outline the approximate construction of a hierarchy of near-resonant N-particle Floquet states. The following phase-space analysis [14], put forward in Sec. IV, shows that the ground state of this hierarchy is tied to a periodic mean-field orbit in precisely the same manner as a Trojan single-particle wave packet is tied to a periodic solution of the corresponding classical equations of motion. The quasiparticle concept then is discussed in Sec. V. Although we do provide the required mathematical details, the main message actually is transported by phase-space portraits which allow one to visualize the correspondence between the N-particle- and the mean-field level. Some possible experimental ramifications are spelled out in the final Sec. VI.

*Electronic address: b.gertjerenken@uni-oldenburg.de

II. MODEL SYSTEM

Within the usual two-mode approximation [15, 16], a Bose-Einstein condensate in a double well potential is described by the Lipkin-Meshkov-Glick Hamiltonian [17]

$$H_0 = -\frac{\hbar\Omega}{2}\left(a_1 a_2^\dagger + a_1^\dagger a_2\right) + \hbar\kappa\left(a_1^\dagger a_1^\dagger a_1 a_1 + a_2^\dagger a_2^\dagger a_2 a_2\right) \ , \tag{1}$$

where Ω is the single-particle tunneling frequency and κ quantifies the strength of the repulsive on-site interaction, such that $2\hbar\kappa$ is the repulsion energy contributed by each pair of Bose particles occuping the same well; the operators $a_j^{(\dagger)}$ (with $j = 1, 2$) annihilate (create) a Boson in well j. We subject this bosonic Josephson junction (1) to a time-periodic drive with amplitude $\hbar\mu_1$ and frequency ω, such that the total Hamiltonian takes the form [12, 13]

$$H(t) = H_0 + \hbar\mu_1 \cos(\omega t)\left(a_1^\dagger a_1 - a_2^\dagger a_2\right) \ . \tag{2}$$

Assuming that the double well is filled with a Bose-Einstein condensate consisting of N particles ($N \gg 1$), the system obviously lives in an $(N+1)$-dimensional Hilbert space $\mathcal{H}_N$, so that its states are specified by vectors with $N+1$ complex components.

Within mean-field theory, one reduces the level of complexity drastically by introducing an order parameter (the "macroscopic wave function") consisting of merely two complex amplitudes, whose absolute squares are supposed to give the fractions of particles found in the two wells [18]. Specifically, let $|L\rangle$ and $|R\rangle$ denote the states associated with the "left" well 1 and with the "right" well 2, respectively. Then the most general single-particle state $|\psi\rangle$ in the space spanned by this two-state basis can be written as

$$|\psi\rangle = \cos(\theta/2)|L\rangle + \sin(\theta/2)\mathrm{e}^{\mathrm{i}\phi}|R\rangle \ , \tag{3}$$

barring an irrelevant overall phase factor. If we assume that this single-particle state be "macroscopically" occupied by N Bosons, the corresponding state vector in $\mathcal{H}_N$, again parametrized by the two angles θ and ϕ, takes the form

$$\begin{aligned} |\theta,\phi\rangle &= \frac{1}{\sqrt{N!}}\left(\cos(\theta/2)a_1^\dagger + \sin(\theta/2)\mathrm{e}^{\mathrm{i}\phi}a_2^\dagger\right)^N |\mathrm{vac}\rangle \\ &= \sum_{n=0}^{N}\binom{N}{n}^{1/2}\cos^n(\theta/2)\sin^{N-n}(\theta/2)\mathrm{e}^{\mathrm{i}(N-n)\phi}|n, N-n\rangle \ , \end{aligned} \tag{4}$$

where $|\mathrm{vac}\rangle$ denotes the vacuum state in $\mathcal{H}_N$, and we have written

$$|n, N-n\rangle = \frac{(a_1^\dagger)^n}{\sqrt{n!}}\frac{(a_2^\dagger)^{N-n}}{\sqrt{(N-n)!}}|\mathrm{vac}\rangle \tag{5}$$

for the Fock state with n particles in the left and $N-n$ particles in the right well. These N-particle states $|\theta,\phi\rangle$ are known as "atomic coherent states"; their properties have been amply discussed in the literature [19].

Given that the mean-field order parameter is in this manner specified by θ and ϕ, one needs their equations of motion. Setting $z = \cos\theta$, it turns out that these two equations of motion coincide with the Hamiltonian equations derived from the classical Hamiltonian function

$$H_{\mathrm{mf}}(z,\phi,\tau) = \frac{N\kappa}{\Omega}z^2 - \sqrt{1-z^2}\cos\phi + \frac{2\mu_1}{\Omega}z\cos\left(\frac{\omega}{\Omega}\tau\right) \tag{6}$$

with dimensionless time $\tau = \Omega t$, in which z plays the role of a momentum and ϕ that of its canonically conjugate position variable; this Hamiltonian function (6) thus describes a nonrigid nonlinear pendulum subjected to an external time-periodic driving force [12, 20].

III. QUANTUM RESONANCE

Because the N-particle Hamiltonian (2) is periodic in time, $H(t) = H(t+T)$ with $T = 2\pi/\omega$, there exists a complete set of Floquet states [21], that is, a set of solutions $|\Psi_m(t)\rangle$ to the time-dependent N-particle Schrödinger equation of the form

$$|\Psi_m(t)\rangle = |u_m(t)\rangle\exp(-\mathrm{i}\varepsilon_m t/\hbar) \quad ; \quad m = 0, 1, \ldots, N \ , \tag{7}$$

with T-periodic Floquet functions $|u_m(t)\rangle = |u_m(t+T)\rangle$ which are complete in $\mathcal{H}_N$ at each instant t. Such a Floquet state (7) reproduces itself after each period T, up to a phase factor determined by its quasienergy ε_m, and therefore can be regarded as an analog of a stationary state. In this section we derive approximations to quite particular, "resonant" Floquet states for the driven bosonic Josephson junction (2) which are N-particle counterparts of the original Trojan wave packets [3–5]. The analysis closely follows an early general sketch by Berman and Zaslavsky [22], and its later extension [9].

We denote the N-particle energy eigenstates of the undriven junction (1) as $|n\rangle$, so that $H_0|n\rangle = E_n|n\rangle$ for $n = 0, 1, \ldots, N$, and assume that the eigenvalues E_n are ordered according to their magnitude. As is well known, under typical conditions the low-energy part of the spectrum, dominated by the tunneling term, is almost harmonic oscillator-like with a slowly decreasing level spacing, whereas the higher-energy part, dominated by the interaction, consists of almost degenerate doublets [11, 12]. Here we choose the driving frequency ω such that

$$E'_r \equiv E_{r+1} - E_r \approx \hbar\omega \tag{8}$$

for a resonant level $n = r$ from the former, nondegenerate part of the spectrum. This resonance condition (8) is the analog of the Trojan condition of equal Kepler and microwave frequency [4]. We then make the Floquet ansatz

$$|\Psi(t)\rangle = \mathrm{e}^{-\mathrm{i}\eta t/\hbar} \sum_n b_n |n\rangle \exp\left[-\frac{\mathrm{i}}{\hbar}\Big(E_r + (n-r)\hbar\omega\Big)t\right] , \tag{9}$$

assuming that the significant contributions to this superposition stem from states close to the resonant one. This produces the system

$$\eta b_n = \Big(E_n - E_r - (n-r)\hbar\omega\Big)b_n + 2\hbar\mu_1 \cos(\omega t) \sum_m \mathrm{e}^{\mathrm{i}(n-m)\omega t} \langle n|J_z|m\rangle b_m \tag{10}$$

for the coefficients b_n, where we have introduced the operator

$$J_z = \left(a_1^\dagger a_1 - a_2^\dagger a_2\right)/2 \tag{11}$$

for the population imbalance between both wells [15, 16]. Expanding the energy eigenvalues E_n quadratically around $n = r$, keeping only the secular terms $m = n \pm 1$, and replacing all matrix elements $\langle n|J_z|n \pm 1\rangle$, somewhat arbitrarily, by the constant $\langle r|J_z|r-1\rangle$, we arrive at the system

$$\eta b_n = \frac{1}{2}(n-r)^2 E''_r b_n + \hbar\mu_1 \langle r|J_z|r-1\rangle \Big(b_{n+1} + b_{n-1}\Big) \tag{12}$$

which couples b_n to its nearest neighbors $b_{n\pm1}$ only. When representing these coefficients as Fourier coefficients of a 2π-periodic function $f(\theta)$ according to

$$b_n = \frac{1}{2\pi} \int_0^{2\pi} \mathrm{d}\theta\, f(\theta) \mathrm{e}^{-\mathrm{i}(n-r)\theta} , \tag{13}$$

this system (12) becomes the Mathieu equation

$$\eta f(\theta) = -\frac{1}{2} E''_r f''(\theta) + 2\hbar\mu_1 \langle r|J_z|r-1\rangle \cos\theta f(\theta) ; \tag{14}$$

substituting $\theta = 2z$ and setting $f(2z) \equiv \chi(z)$ yields its standard form [23]

$$\left(\frac{\mathrm{d}^2}{\mathrm{d}z^2} + \alpha - 2q\cos(2z)\right)\chi(z) = 0 \tag{15}$$

with parameters

$$\alpha = \frac{8\eta}{E''_r} , \tag{16}$$

$$q = \frac{4}{E''_r/(\hbar\omega)} \frac{2\mu_1}{\omega} \langle r|J_z|r-1\rangle . \tag{17}$$

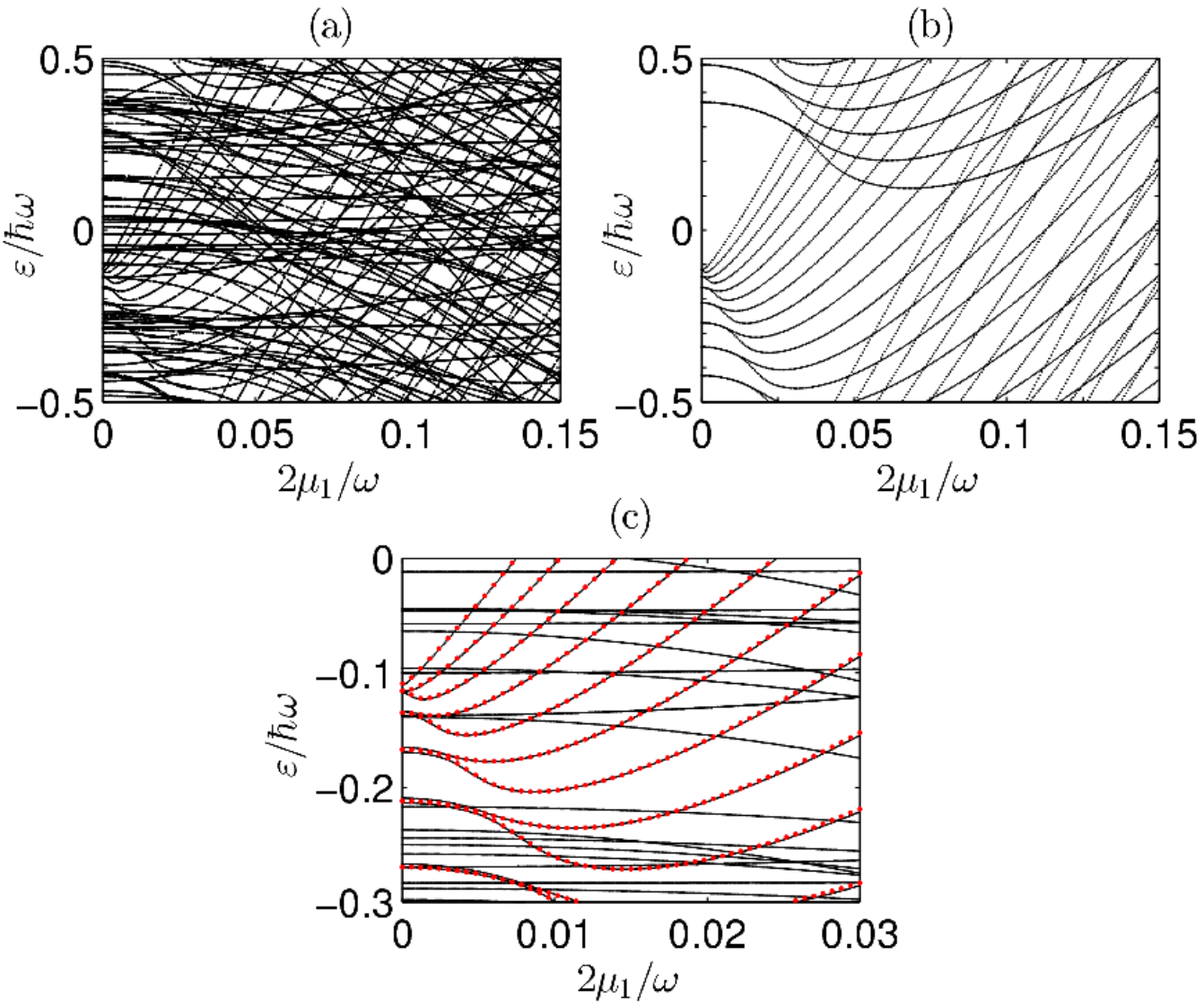

FIG. 1: Quasienergies for the driven bosonic Josephson junction (2) with $N = 100$ particles, scaled interaction strength $N\kappa/\Omega = 1.9$, and scaled driving frequency $\omega/\Omega = 1.6$. (a) Numerically computed, exact complete spectrum, showing quasienergies of both near-resonant and non-resonant states. (b) Quasienergies of near-resonant states with $k = 0, \ldots, 18$ according to the approximation (20). Here $r = 34$ is the resonant state of the undriven junction; the Mathieu parameter (17) is given by $q\omega/2\mu_1 = 5402$. (c) Exact quasienergies (black lines) compared to the approximate ones (red dots) for small scaled driving strengths $2\mu_1/\omega$. Additional lines stem from non-resonant states.

The requirement that $\chi(z) = \chi(z + \pi)$ be a π-periodic Mathieu function then restricts α to one of the discrete characteristic values

$$\alpha_k(q) = \begin{cases} a_k(q) & \text{for} \quad k = 0, 2, 4, \ldots \\ b_{k+1}(q) & \text{for} \quad k = 1, 3, 5, \ldots \end{cases}, \tag{18}$$

as tabulated in the mathematical literature [23]. Writing $f_{\ell,k}$ for the ℓth Fourier coefficient of the Mathieu function singled out by $\alpha_k(q)$, one thus has the approximations

$$|\Psi_k(t)\rangle = \exp\left(-\frac{\mathrm{i}}{8\hbar}E_r''\alpha_k t\right)\sum_\ell f_{\ell,k}|r+\ell\rangle \exp\left[-\frac{\mathrm{i}}{\hbar}\Big(E_r + \ell\hbar\omega\Big)t\right] \tag{19}$$

for near-resonant Floquet states; their quasienergies

$$\varepsilon_k = E_r + \frac{1}{8} E_r'' \alpha_k(q) \mod \hbar\omega \tag{20}$$

are determined by the Mathieu characteristic values (18). In comparison with the exact spectrum depicted in Fig. 1, computed numerically by diagonalizing the one-cycle time evolution operator $U(T,0)$, this approximation performs quite well for moderate scaled driving strengths $2\mu_1/\omega$; the regular fan of quasienergies described by Eq. (20) is well discernible against a background of further quasienergies stemming from non-resonant states. Interestingly, the many-body Floquet states (19) carry a new quantum number $k = 0, 1, 2, \ldots$, but at this point the physical significance of this quantum number does not seem to be obvious. In the following section these states (19) will be interpreted from the mean-field point of view; in particular, it will be shown that the state with $k = 0$ has Trojan properties.

IV. N-PARTICLE – MEAN FIELD CORRESPONDENCE

In a semiclassical approach, the quantum states of a one-dimensional oscillator with corresponding classical momentum p and conjugate coordinate x are characterized by the Bohr-Sommerfeld condition

$$\frac{1}{2\pi} \oint_{\gamma_k} p \mathrm{d}x = \hbar \left(k + \frac{1}{2} \right) \tag{21}$$

with integer $k = 0, 1, 2, \ldots$, assuming that the classical oscillation has two "soft" turning points so that the Maslov index of the invariant curve γ_k in phase space $\{(p, x)\}$ is $\mathrm{ind}\, \gamma_k = 2$: This condition (21) singles out those invariant curves from which the discrete quantum states are obtained by means of the usual WKB construction [24]. An appropriately adapted procedure yields the Floquet states of a T-periodically forced oscillator, provided the classical motion is integrable: In this case one has T-periodic tubes in the extended phase space $\{(p, x, t)\}$ also incorporating the time t which are invariant under the Hamiltonian flow. Then a first quantization condition of the form (21), with a path γ_k winding once around such an invariant tube at fixed time t, selects the desired tubes which are associated with the Floquet wave functions, whereas a second condition, with a T-periodic path led along the respective tube, enables one to compute their quasienergies [25].

One can apply these deliberations to the classical nonlinear driven pendulum (6), having been obtained as the mean-field approximation to the N-particle system (2), and "re-quantize" this classical pendulum in order to obtain an effective single-particle description. To this end, one merely has to observe that the "momentum" variable $z = \cos\theta = \cos^2(\theta/2) - \sin^2(\theta/2)$ directly corresponds, by means of the parametrization (3), to the operator $2J_z/N$, with J_z as defined by Eq. (11); note that J_z actually is the third component of a set of three operators J_x, J_y, J_z satisfying angular-momentum commutation relations [15, 16]. This implies that the standard formula (21) here takes the form

$$\frac{1}{2\pi} \oint_{\gamma_k} z \mathrm{d}\phi = \hbar_{\mathrm{eff}} \left(k + \frac{1}{2} \right) \tag{22}$$

with the effective Planck constant

$$\hbar_{\mathrm{eff}} = \frac{2}{N} \tag{23}$$

which equals twice the inverse particle number. However, while the classical pendulum (6) is *integrable* when $2\mu_1/\omega = 0$, so that the semiclassical quantization produces approximations to all its energy eigenstates, it becomes non-integrable, and partly *chaotic*, when the driving force is turned on. This is clearly visible in the Poincaré surfaces of section shown in Fig. 2, obtained as stroboscopic plots from exact solutions to the classical equations of motion [26]. In accordance with the Poincaré-Birkhoff theorem [24], a new stable elliptic fixed point, corresponding to a stable T-periodic orbit, emerges for weak driving strength when the oscillation frequency of the unperturbed pendulum equals the driving frequency; this fixed point lies in the center of the banana-shaped resonance zone appearing in panel (b). When increasing $2\mu_1/\omega$, this resonance zone grows until it becomes an island of mainly regular motion embedded in the chaotic sea shown in panel (d) — a standard scenario in Hamiltonian systems. The invariant curves surrounding the central fixed point of the resonant island constitute sections of invariant T-periodic flow tubes with a plane of constant time, and thus provide the quantization paths γ_k required by Eq. (22) for computing semiclassical approximations to the N-particle Floquet states [8, 25]. Evidently this procedure now can only yield the "resonant" Floquet states carried by the island, not covering the states associated with the chaotic sea. However, it needs to be stressed that even the apparently regular island actually exhibits self-similar chaotic motion on fine scales [24], so

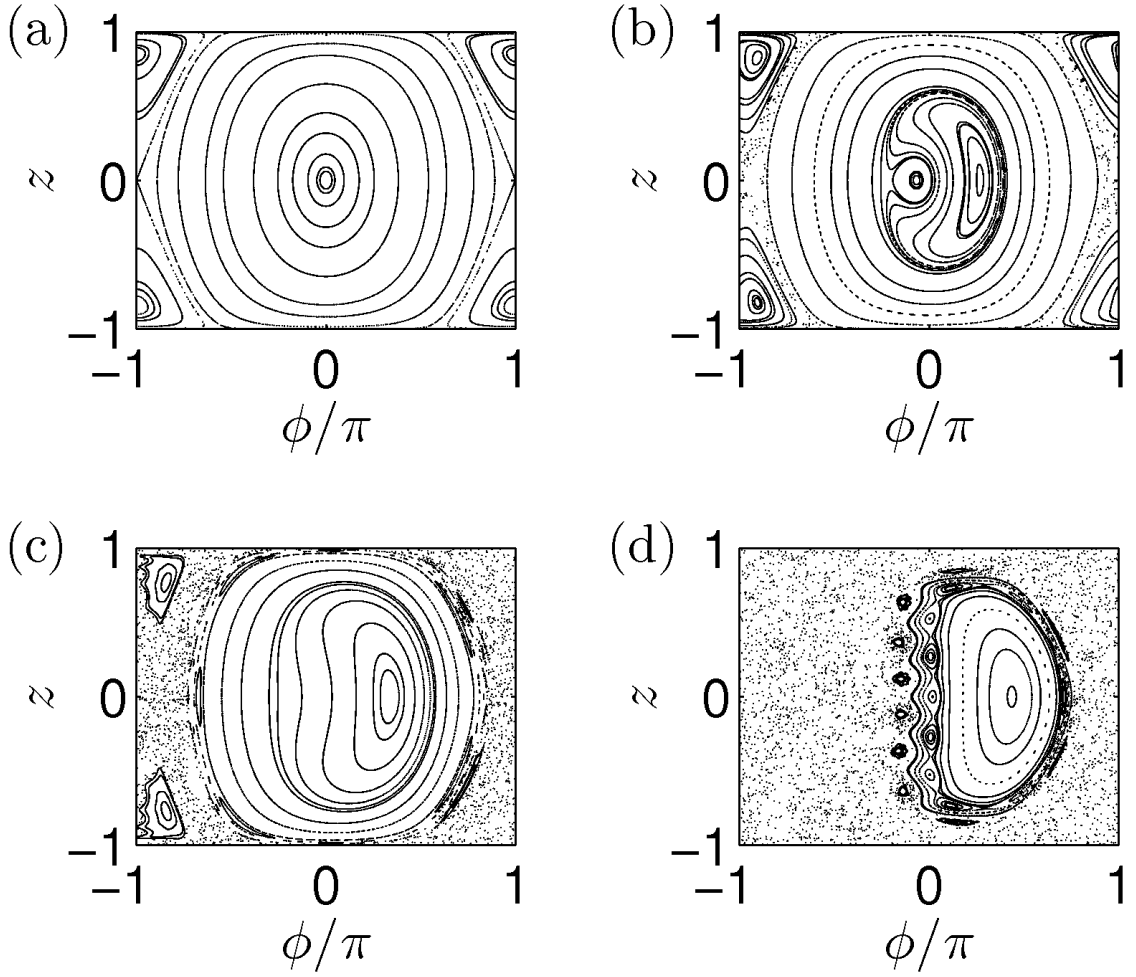

FIG. 2: Poincaré surfaces of section for the nonrigid classical pendulum (6), for $N\kappa/\Omega = 0.95$ and $\omega/\Omega = 1.62$. The driving strengh $2\mu_1/\omega$ is given by 0 (a), 0.02 (b), 0.1 (c), and 0.3 (d). Observe the emergence and growth of a resonance zone surrounding a stable (elliptic), $2\pi/\omega$-periodic orbit. While the integrability of the unperturbed pendulum is reflected in the regularity of the section (a), the non-integrability of the driven system manifests itself in a chaotic sea emanating from the separatix curve of the undriven motion. In these and all following sections, initial conditions are chosen such that all relevant features become visible.

that here the Bohr-Sommerfeld rule (22) applies in a coarse-grained sense, glossing over the unresolved details. This will turn out to be important in Sec. V.

These considerations highlight the particular conceptual value of the driven bosonic Josephson junction (2): It allows one to invoke techniques previously developed in the investigation of the quantum-classical correspondence for studying the relation between full quantum N-particle dynamics and its mean-field description [27, 28], with the large-system limit $N \to \infty$ paralleling, in view of Eq. (23), the semiclassical limit $\hbar \to 0$.

In the absence of a time-periodic force, that is, for $2\mu_1/\omega = 0$, the semiclassical quantization of the nonrigid pendulum (6) has been explored in significant detail by a large number of authors [14, 29–33]. The viability of this approach is underlined by Fig. 3: Here we take $N = 20$ and depict Husimi distributions

$$\mathcal{Q}_k^{(N)}(z,\phi) = \left|\langle\theta,\phi|\Psi_k^{(N)}\rangle\right|^2 , \tag{24}$$

i.e., squared projections of the exact kth N-particle energy eigenstate $|\Psi_k^{(N)}\rangle$ of the undriven bosonic Josephson junction (1) onto the atomic coherent states (4), being superimposed on the corresponding Poincaré surface of section of the classical pendulum with $z = \cos\theta$. Better than any lengthy verbose explanation, this figure shows how Eq. (22) works: The exact energy eigenstates states are semiclassically attached to the invariant curves selected by this very condition. As emphasized by Mahmud, Perry, and Reinhard, the semiclassical re-quantization gives fairly good

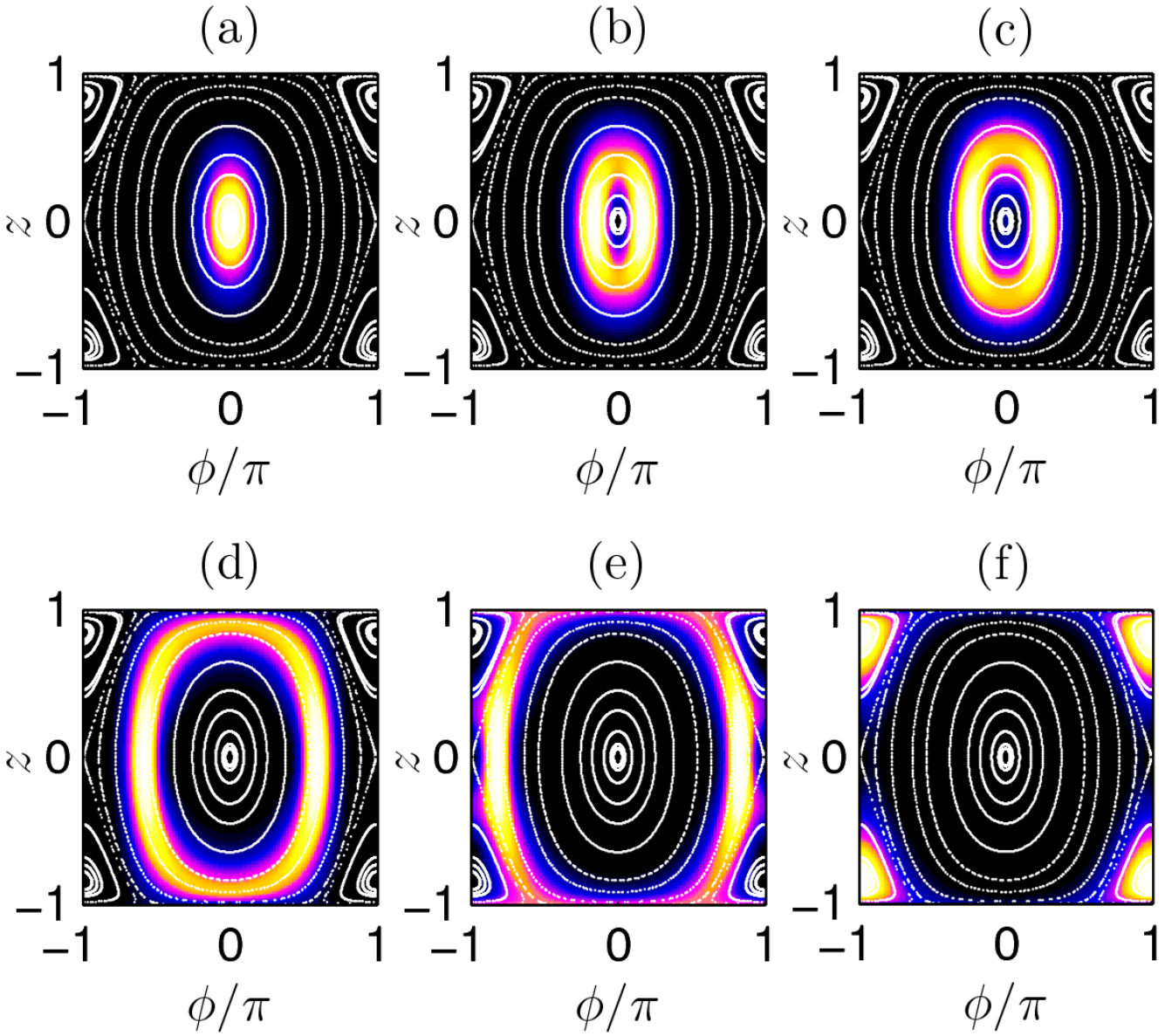

FIG. 3: Color-coded Husimi distributions (24) of exact kth N-particle energy eigenstates of the undriven bosonic Josephson junction (1) with $N = 20$ and $N\kappa/\Omega = 0.95$, superimposed on the corresponding phase-space portrait of the classical nonrigid pendulum (6) taken from Fig. 2(a). Brighter colors amount to larger values of the Husimi distribution. Quantum numbers k of the states considered are $0, 1, 2, 10, 15, 20$ [(a)-(f)].

quantitative results even when the particle number N is quite small, so that $\hbar_{\rm eff}$ still is comparatively large [14].

In order to extend this procedure for obtaining a semiclassical understanding of the Floquet states of the driven bosonic Josephson junction (2), one only has to compare the Husimi distributions of exact, numerically computed N-particle Floquet states $|\Psi_k^{(N)}(t_0)\rangle$ with the corresponding Poincaré sections of the driven pendulum (6), taken at times t_0 mod T. In Fig. 4 we show such comparisons for the conditions of Fig. 2(d), again taking $N = 20$. Clearly, the regular island supports Floquet states which are attached to its invariant curves, arising as sections of invariant tubes, exactly as required by the quantization condition (22). The key point here is that this observation leads to a natural explanation of the quantum number k found in Sec. III as a result of the Mathieu analysis: The quantum numbers k assigned to the exact near-resonant Floquet states by enumerating their quasienergies, which are well approximated by the Mathieu expression (20), *agree* with the quantum numbers k assigned to them on the grounds

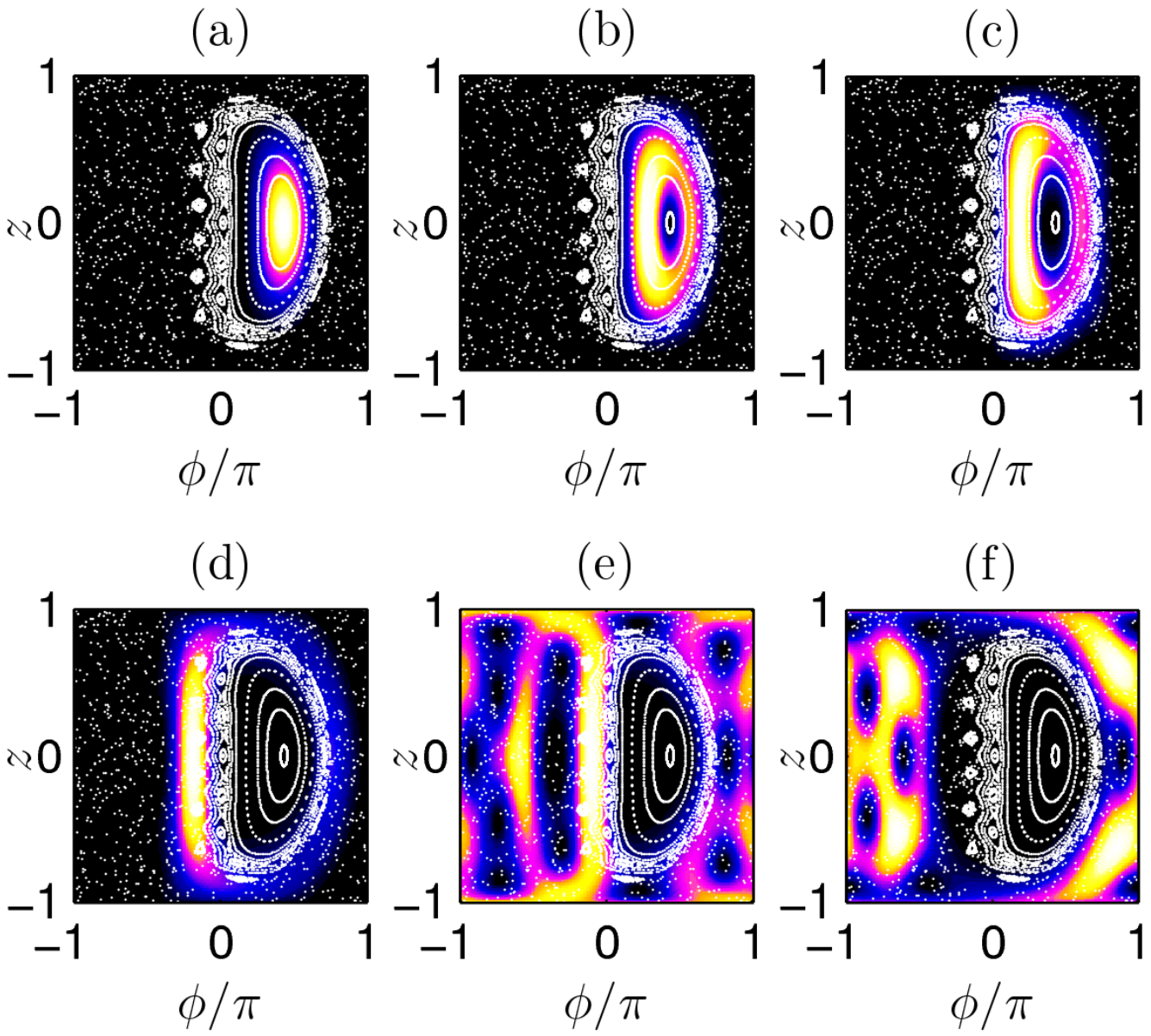

FIG. 4: Color-coded Husimi distributions (24) of exact kth near-resonant N-particle Floquet states of the driven bosonic Josephson junction (2) with $N = 20$, $N\kappa/\Omega = 0.95$, $\omega/\Omega = 1.62$, and $2\mu_1/\omega = 0.3$, superimposed on the corresponding Poincaré surface of section taken from Fig. 2(d). Quantum numbers k, determined according to the Mathieu approximation (20), are $0, 1, 2, 6$ [(a)-(d)]. Panels (e) and (f) display Husimi distributions of Floquet states associated with the stochastic sea.

of the Bohr-Sommerfeld formula (22). In particular, the ground state-like Floquet state with $k = 0$ is semiclassically associated with the innermost quantized invariant tube surrounding the stable T-periodic orbit. Precisely the same connection holds in the case of the nonspreading Rydberg Trojan wave packets [3, 4], which again can be semiclassically interpreted as ground states of a quantized resonance [8, 10]. Thus, the resonant Floquet state with $k = 0$ of a driven bosonic Josephson junction constitutes a many-particle counterpart of a Rydberg Trojan state.

These deliberations also imply that the resonant eigenstate $n = r$ of the undriven Josephson junction (1) is adiabatically transformed into the Trojan state $k = 0$ when the external drive is turned on. Fig. 5 illustrates this metamorphosis for the set of parameters employed so far, while Fig. 6 shows the reverse transformation of the unperturbed ground state into an excitation $k > 0$ of the Trojan.

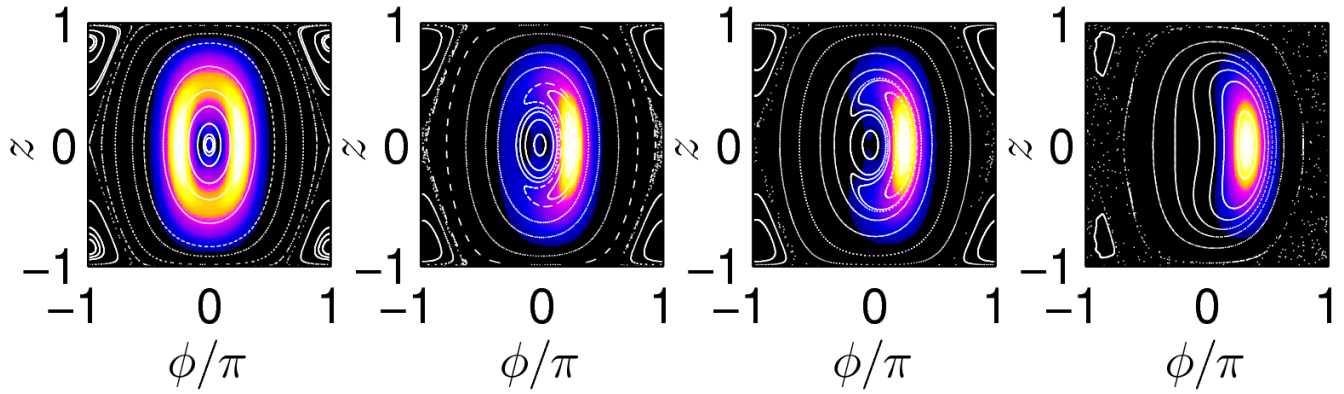

FIG. 5: Adiabatic transformation of the eigenstate $n = 2$ of the undriven bosonic Josephson junction (1), which is resonant $(2 = r)$ when $N = 20$, $N\kappa/\Omega = 0.95$, and $\omega/\Omega = 1.62$, into the Trojan Floquet state $k = 0$. From left to right, scaled driving amplitudes $2\mu_1/\omega$ are 0.0, 0.005, 0.01, 0.1.

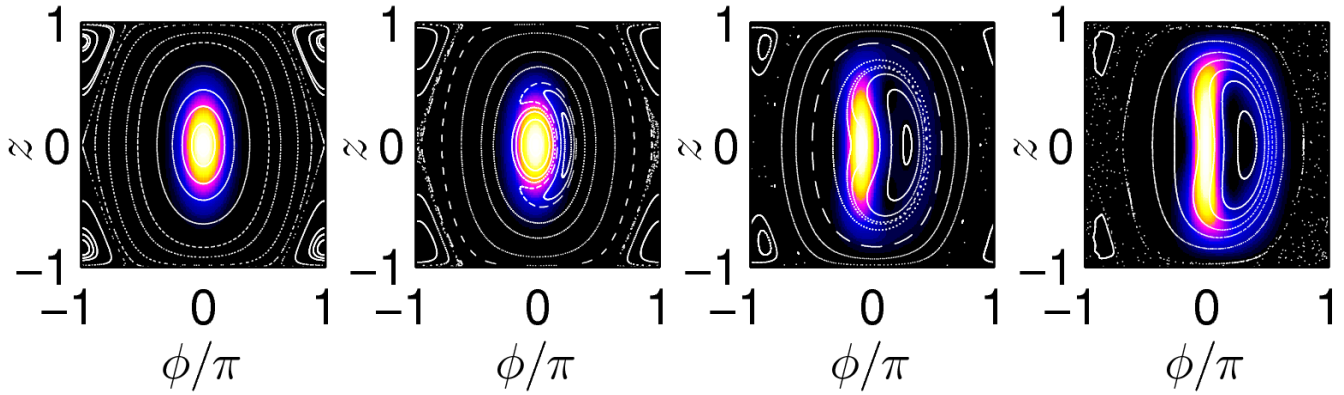

FIG. 6: Adiabatic transformation of the ground state of the undriven bosonic Josephson junction (1) into a near-resonant Floquet state with $k = 2$, for the same parameters as in Fig. 5. From left to right, scaled driving amplitudes $2\mu_1/\omega$ here are 0.0, 0.005, 0.04, 0.1.

V. THE "FLOTON" QUASIPARTICLE

The small particle number $N = 20$ had been chosen in the previous section mainly for illustrative purposes, but with respect to topical laboratory experiments [11] particle numbers on the order of 1000 are more to the point. Therefore, Fig. 7 shows the evolution of a Trojan with $N = 1000$ in time, again under the conditions of the Poincaré section displayed in Fig. 2(d). Here the scaling dictated by the effective Planck constant (23) manifests itself in a striking manner: In comparison with Fig. 4, where $\hbar_{\rm eff} = 0.1$, one now has $\hbar_{\rm eff} = 0.002$, implying that the Trojan Floquet state $k = 0$ here is associated with a flow tube much closer to the elliptic periodic orbit than it was in Fig. 4, so that its Husimi distribution appears to be sharply centered around this orbit. By the same token, the resonant island now can carry more near-resonant Floquet states with $k > 0$, and the Floquet states can resolve much finer details of phase space; this is illustrated by the Husimi distributions of further representative Floquet states, both near-resonant and non-resonant ones, collected in Fig. 8.

The Trojan state displayed in Fig. 7 represents an exact collective response mode of Bose particles in the driven double-well potential which is quite particular in several respects. Firstly, it is "nonspreading in phase space", being semiclassically attached to a T-periodic tube remaining invariant under the Hamiltonian flow, and therefore it does not heat up in the course of time despite the action of the time-periodic drive. Secondly, it behaves like a single particle — namely, the fictitious particle trapped in the ground state $k = 0$ described by the Mathieu equation (14), which

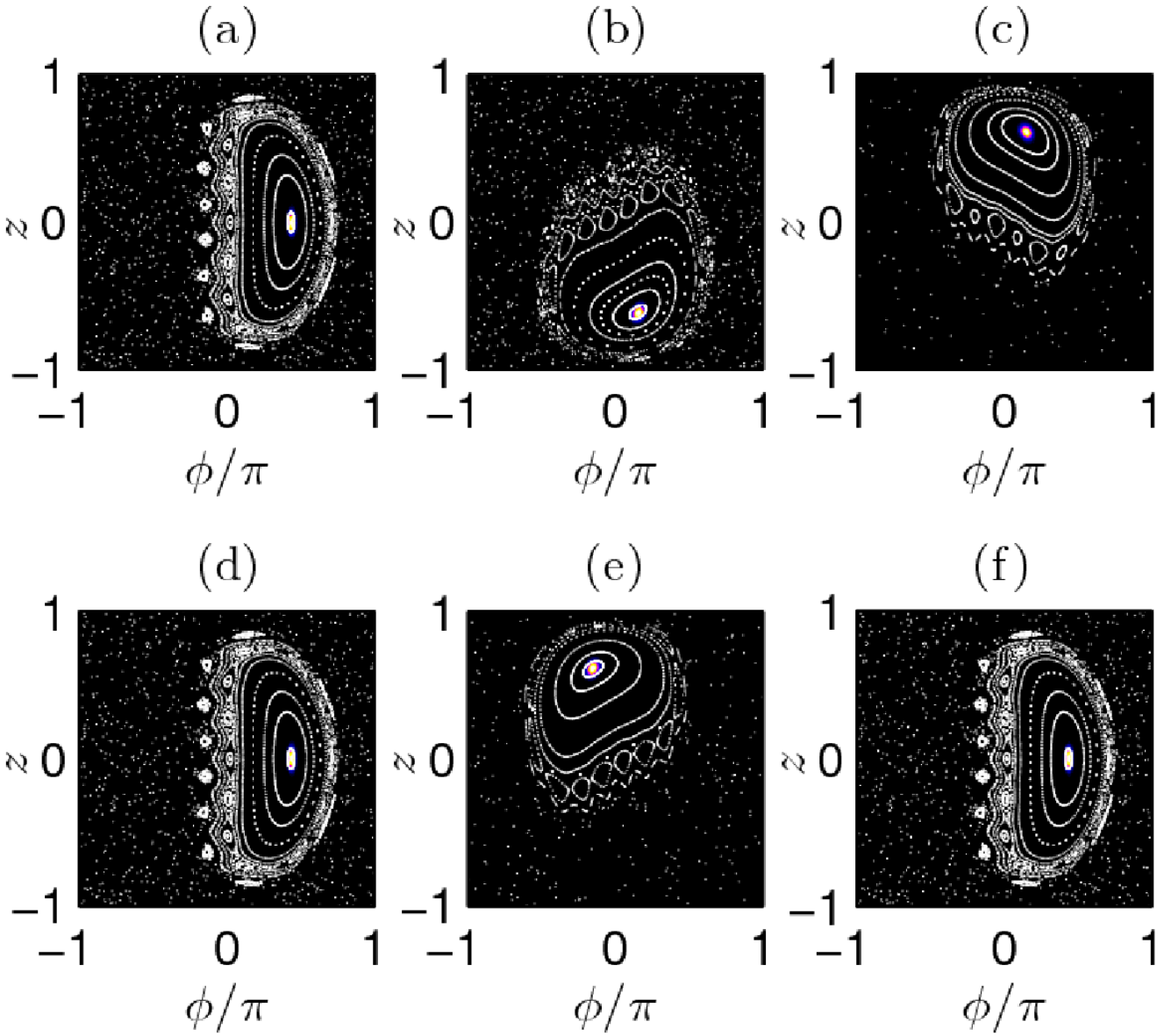

FIG. 7: Evolution of the Trojan Floquet state $k = 0$ for $N = 1000$ in time; the other parameters are as in Fig. 4. Observe that the Husimi distribution is narrowly centered around the periodic orbit, illustrating the scaling implied by the effective Planck constant $\hbar_{\rm eff} = 2/N$. Poincaré sections are taken at times t/T equal to $0.0, 0.2, 0.8, 1.0, 5.7, 10.0$ [(a)-(f)]. This many-body state provides a prototypical example of a floton quasiparticle, being the state with the *highest* degree of coherence recorded in Fig. 9. The long-time evolution monitored in panel (f) testifies its periodicity.

is an effective Schrödinger equation for a (quasi-)particle in a cosine well with periodic boundary conditions, having led to the Floquet-Mathieu approximation (19). Such quasiparticles have been named "flotons" in Ref. [9]. In this sense, the many-particle analog of a nonspreading Rydberg Trojan wave packet is a nonheating floton quasiparticle; this quasiparticle possesses a well-defined discrete set of excited states with $k > 0$.

While most of the arguments employed in the previous section are nothing but immediate adaptions of tools routinely used in the discussion of the correspondence between quantum and classical systems [24], there is one feature which does not occur in that well-established field, but deserves particular attention. In our case the classical system (6) is not given "as such", but emerges only as a mean-field description of a quantum many-particle system. The reduction of the latter to the mean-field level does not constitute a systematic approximation, but involves the uncontrolled factorization of expectation values of products of operators into products of expectation values of individual operators [18]. Thus, it cannot be taken for granted that the solution of the mean-field equations of motion

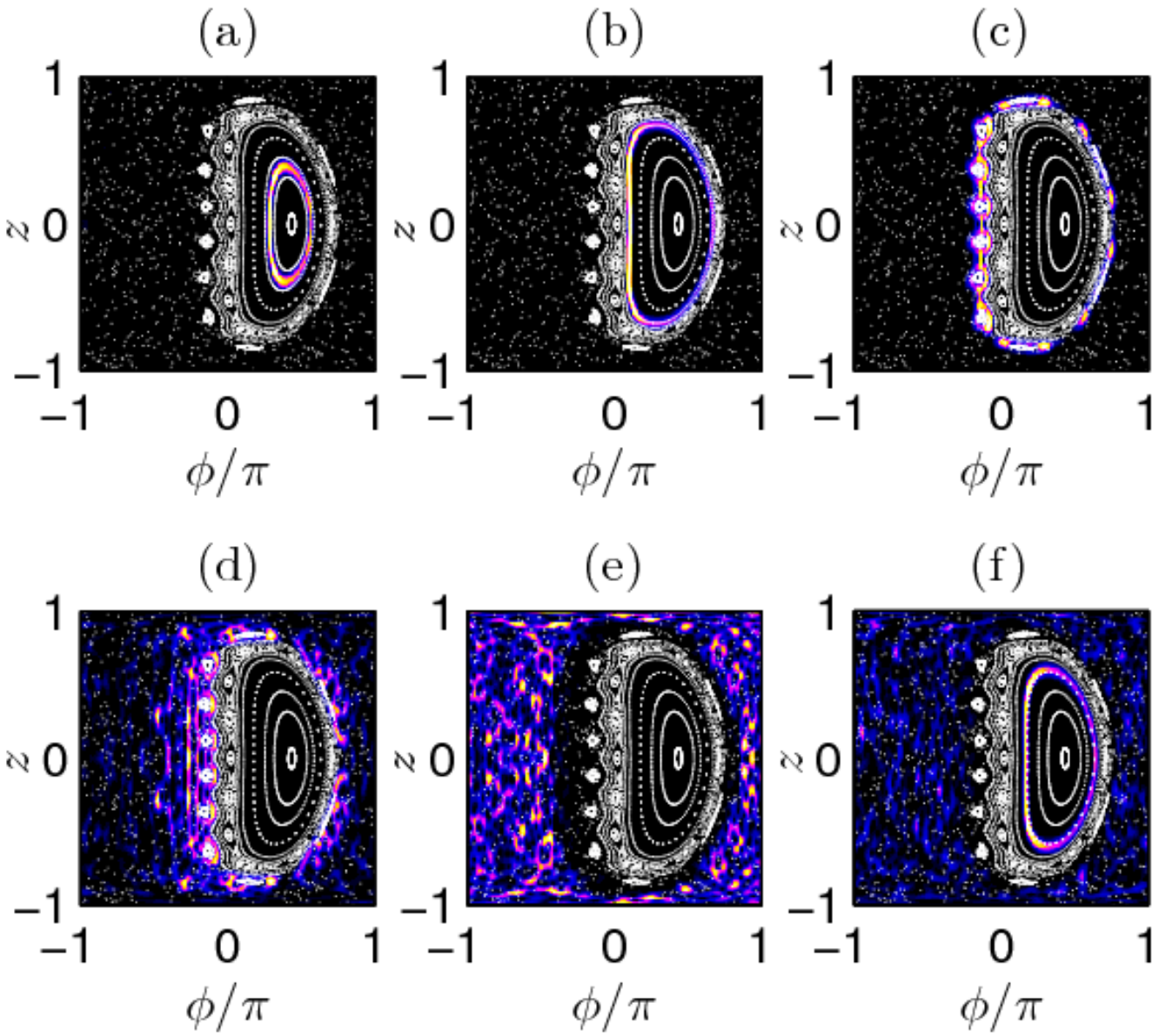

FIG. 8: Husimi distributions of further exact Floquet states for $N = 1000$; the system parameters are the same as in Figs. 4 and 7. Evidently these states are semiclassically associated with the central resonant island (a,b), with the surrounding chains of higher-order islands (c,d), or with the chaotic sea (e). The state depicted in (f) is a hybrid state, being linked to both an invariant curve within the island and to the chaotic sea; incidentally, this is the state with the *lowest* degree of coherence recorded in Fig. 9.

actually "corresponds" to the dynamics of the N-particle system. Indeed, as discussed in technical detail by Castin and Dum, one expects depletion of the condensate when the solution to the mean-field equations of motion tends to become chaotic [34]. Essentially, the reduction of the full N-particle dynamics, here being given in terms of vectors with $N + 1$ complex components, to the mean-field level with its two-component order parameter is viable only if the N-particle original is sufficiently simple, or ordered, in the sense that it has the form (4) of an N-fold occupied single-particle state at least to a good aproximation. Otherwise the descent to the mean-field level is thwarted by a drastic loss of information — if there is no order, there is no order parameter. Under conditions such that the N-particle quantum system does not admit the introduction of an order parameter, one can of course still solve the mean-field equations of motion, but the solutions acquire a meaning which is different from those cases where an order parameter actually does exist.

Therefore, it is necessary to quantify the "simplicity" of an N-particle quantum system, amounting to its "degree of

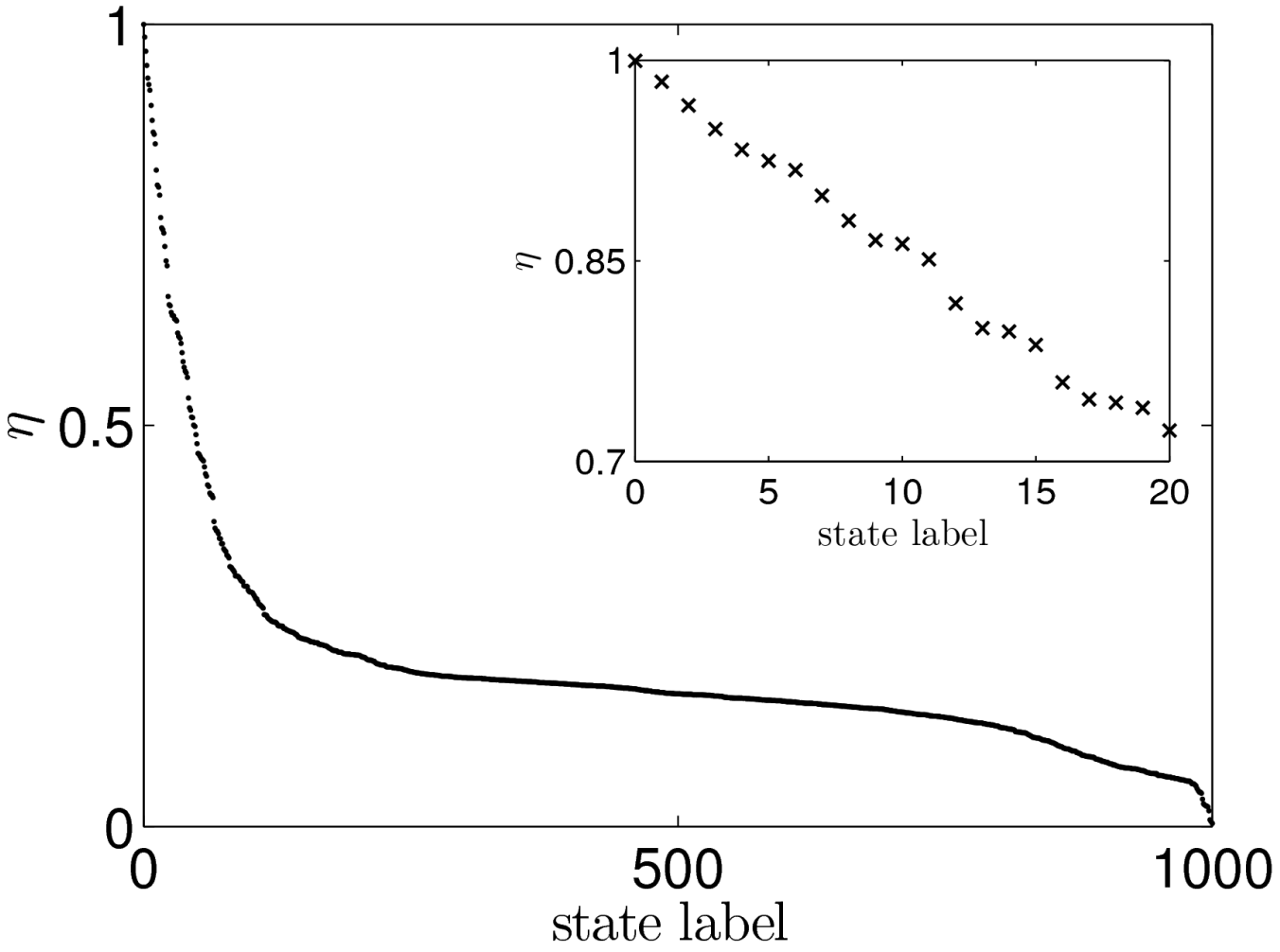

FIG. 9: Degree of coherence η, as defined by Eq. (26), for all 1001 Floquet states furnished by the driven Josephson junction (2) with parameters as in Figs. 7 and 8. States are ordered with respect to decreasing magnitude of η. The highest value $\eta_{\max} = 0.9997$, signaling close-to-perfect mean-field approximability, is attained by the floton inspected in Fig. 7; the lowest value $\eta_{\min} = 0.0038$ is provided by the hybrid state shown in Fig. 8(f).

mean-field approximability", or coherence. Such information is contained in the one-particle reduced density matrix ϱ, which, in the particular case of our two-mode model, adopts the form

$$\varrho = \begin{pmatrix} \langle a_1^\dagger a_1 \rangle & \langle a_1^\dagger a_2 \rangle \\ \langle a_2^\dagger a_1 \rangle & \langle a_2^\dagger a_2 \rangle \end{pmatrix} , \tag{25}$$

the expectation values being taken with respect to the quantum state under investigation. Obviously the invariant trace of ϱ, which is the sum of its two eigenvalues, equals the total particle number N. If the larger eigenvalue alone already is close to N, then ϱ approaches a projection operator, times N, onto the associated eigenvector. This indicates that there exists a simple condensate, *i.e.*, an almost N-fold occupied single-particle state constituting the order parameter. In the other extreme where both eigenvalues are close to $N/2$ the condensate is fragmented. Hence, Leggett has introduced the "degree of simplicity" (coherence)

$$\eta = 2N^{-2} \operatorname{tr} \varrho^2 - 1 \tag{26}$$

which is computed from the trace of the squared single-particle density matrix [18]: Its maximum value $\eta = 1$ indicates a perfect condensate guaranteeing optimal mean-field approximability, whereas the minimum value $\eta = 0$ signals maximal fragmentation.

It is, therefore, of interest to inspect the simplicity η of the Floquet states provided by the driven Josephson junction (2), in order to assess the relevance of the chaotic classical mean-field solutions. In Fig. 9 we plot η for

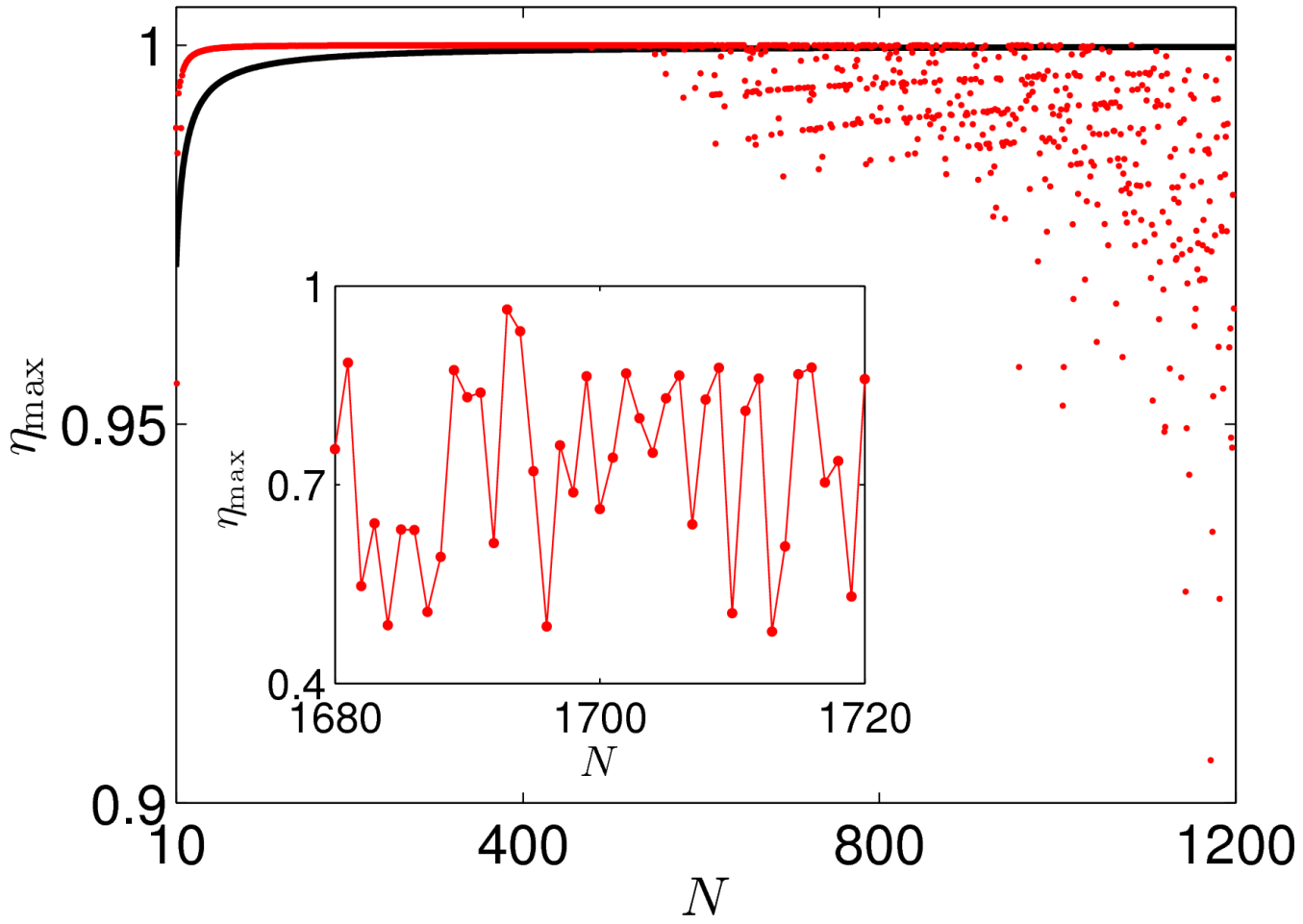

FIG. 10: Red dots: Maximum degree of coherence $\eta_{\max}$, taken over all respective Floquet states, as function of the particle number N. Once again, the system parameters are $N\kappa/\Omega = 0.95$, $\omega/\Omega = 1.62$, and $2\mu_1/\omega = 0.3$. For comparison, the black line shows $\eta_{\max}$ for the nondriven junction. Observe the scale of the inset!

all 1001 Floquet states which arise for the parameters of Figs. 7 and 8. This calculation reveals the third characteristic feature of the floton: Under ideal conditions, as met here, it gives rise to a value of η which is quite close to one, and thus possesses close-to-perfect mean-field approximability. The excited states with $k > 0$ carried by the resonant island are responsible for the rapidly decreasing leftmost part of the plot, while the states mainly associated with the chaotic sea lead to the extended plateau; some hybrid states, such as the one exemplified by Fig. 8(f), carry a particularly low value of η.

It is with regard to this pertinent problem of mean-field approximability that the further investigation of many-body Trojan states, *i.e.*, of flotons, may bear some significance. Since such states can be generated by adiabatic following, as witnessed by Fig. 5, they should be experimentally accessible. One key question then is to what extent the features extracted from our model system do survive in experimentally realistic set-ups, which in general will be way too sophisticated to admit full N-particle modeling, but for which mean-field calculations may still be feasible. Here the knowledge that floton-like mean-field solutions do indeed have a faithful N-particle counterpart would be quite valuable. However, there is still another catch. Namely, with increasing particle number N and correspondingly decreasing effective Planck constant $\hbar_{\text{eff}} = 2/N$ the system is able to explore its phase space on ever finer scales, and ultimately "feels" that the resonant island does not represent perfectly integrable dynamics, but rather is subject to the Kolmogorov-Arnold-Moser (KAM) scenario: The invariant flow tubes with not sufficiently irrational winding numbers are destroyed [24]. But this means that, in a strict mathematical sense, the question arises whether or not the quantization curves γ_k required by the naive Bohr-Sommerfeld condition (22) actually are available — if not, the order parameter should be degraded. Since the answer to this question depends sensitively on the precise value of $\hbar_{\text{eff}}$, and therefore on the precise particle number N, one has to expect strong fluctuations of the system's coherence under small variations of N, once N becomes sufficiently large.

This expectation is confirmed in an impressive manner by Fig. 10, which shows the respective maximum $\eta_{\max}$ of the η-values of all Floquet states provided by the driven junction (2) for a prescribed value of N, again for the same set of system parameters as employed before. Indeed, at about $N \approx 500$ fluctuations of $\eta_{\max}$ start to make themselves felt, and become more pronounced with increasing N; the previous observation that $\eta_{\max}$ is close to unity for $N = 1000$ now appears as a fortuitous coincidence. In contrast, such fluctuations do not occur for the undriven junction (1), which merely gives rise to exactly integrable mean-field dynamics.

Such fluctuations of the order parameter constitute the fourth, and probably most important property of the floton, and lead to a hard, testable prediction: In a set of experiments with resonantly driven Bose-Einstein condensates, prepared under ostensibly identical conditions but still admitting a small uncertainty of the large particle number, there should be large shot-to-shot fluctuations of the condensate fraction.

VI. EXPERIMENTAL IMPLICATIONS

Quantum resonances, as sketched in Sec. III, constitute a generic feature of driven nonlinear systems. Therefore, the appearance of Trojan quasiparticles which correspond, to good approximation, to an N-fold occupied time-periodic single-particle state is not restricted to the somewhat idealized model system (2). In particular, one may deliberately "engineer" such a resonance in an anharmonic single-well trapping potential which is combined with additional time-periodic forcing. A central question then is how such time-dependent condensates could be prepared. Here a further insight becomes important: As emphasized by Leggett [18], the tendency to undergo Bose-Einstein condensation into a "macroscopically" occupied single-particle state is not restricted to states of thermal equilibrium. Rather, it can be understood as a consequence of two mutually reinforcing effects: On the one hand, bosonic configurations in which many particles occupy the same single-particle orbital have a higher statistical weight than in the classical case; on the other, the Hartree-Fock energy of two identical spinless bosons in different single-particle orbitals is greater than that of two such bosons in the same orbital [18]. Hence, one may reasonably assume that a resonantly driven Bose gas condenses "by itself" into the floton ground state $k = 0$ when the parameters are chosen such that this Floquet state becomes the one with the lowest mean energy. If so, the floton would manifest itself, *e.g.*, as a clearly discernible condensate peak in a time-of-flight recording, at least as long as the particle number is not too large. Because of the nonheating property, this signature should persist even after comparatively long driving times. But the true "smoking gun" ultimately betraying the floton might consist in fluctuations of the kind depicted in Fig. 10: If the average particle number exceeds a certain value depending on the specific set-up, the height of the condensate peak observed in a series of time-of-flight experiments would fluctuate in a seemingly erratic manner from measurement to measurement.

Acknowledgments

We acknowledge discussions with C. Weiss. This work was supported by the Deutsche Forschungsgemeinschaft (DFG) under grant no. HO 1771/6-2. The computations were performed on the HPC cluster HERO, located at the University of Oldenburg and funded by the DFG through its Major Research Instrumentation Programme (INST 184/108-1 FUGG), and by the Ministry of Science and Culture (MWK) of the Lower Saxony State.

[1] P. Robutel and J. Souchay, in *Dynamics of Small Solar System Bodies and Exoplanets*. Lecture Notes in Physics **790** (Springer, Berlin, 2010), p. 197.
[2] M. Connors, P. Wiegert, and C. Veillet, Nature **475**, 481 (2011).
[3] I. Bialynicki-Birula, M. Kaliński, and J. H. Eberly, Phys. Rev. Lett. **73**, 1777 (1994).
[4] M. Kalinski and J. H. Eberly, Phys. Rev. A **53**, 1715 (1996).
[5] M. Kalinski and J. H. Eberly, Opt. Express **1**, 216 (1997).
[6] H. Maeda and T. F. Gallagher, Phys. Rev. Lett. **92**, 133004 (2004).
[7] B. Wyker, S. Ye, F. B. Dunning, S. Yoshida, C. O. Reinhold, and J. Burgdörfer, Phys. Rev. Lett. **108**, 043001 (2012).
[8] J. Henkel and M. Holthaus, Phys. Rev. A **45**, 1978 (1992).
[9] M. Holthaus, Chaos, Solitons & Fractals **5**, 1143 (1995).
[10] A. Buchleitner, D. Delande, and J. Zakrzewski, Phys. Rep. **368**, 409 (2002).
[11] R. Gati and M. K. Oberthaler, J. Phys. B: At. Mol. Opt. Phys. **40**, R61 (2007).
[12] M. Holthaus and S. Stenholm, Eur. Phys. J. B **20**, 451 (2001).
[13] T. Jinasundera, C. Weiss, and M. Holthaus, Chem. Phys. **322**, 118 (2006).

[14] K. W. Mahmud, H. Perry, and W. P. Reinhardt, Phys. Rev. A **71**, 023615 (2005).
[15] G. J. Milburn, J. Corney, E. M. Wright, and D. F. Walls, Phys. Rev. A **55**, 4318 (1997).
[16] S. Raghavan, A. Smerzi, and V. M. Kenkre, Phys. Rev. A **60**, R1787 (1999).
[17] H. J. Lipkin, N. Meshkov, and A. J. Glick, Nucl. Phys. **62**, 188 (1965).
[18] A. J. Leggett, Rev. Mod. Phys. **73**, 307 (2001).
[19] F. T. Arecchi, E. Courtens, R. Gilmore, and H. Thomas, Phys. Rev. A **6**, 2211 (1972).
[20] A. Smerzi, S. Fantoni, S. Giovanazzi, and S. R. Shenoy, Phys. Rev. Lett. **79**, 4950 (1997).
[21] J. H. Shirley, Phys. Rev. **138**, B979 (1965).
[22] G. P. Berman and G. M. Zaslavsky, Phys. Lett. A **61**, 295 (1977).
[23] M. Abramowitz and I. A. Stegun (Eds.), *Handbook of Mathematical Functions* (Dover, New York, 1972), ch. 20.
[24] M. C. Gutzwiller, *Chaos in Classical and Quantum Mechanics* (Springer-Verlag, New York, 1990).
[25] H. P. Breuer and M. Holthaus, Ann. Phys. (N.Y.) **211**, 249 (1991).
[26] We solve all differential equations, both classical and quantum mechanical ones, by means of a variable-order Adams PECE method: See L. F. Shampine and M. K. Gordon, *Computer Solution of Ordinary Differential Equations* (Freeman and Company, San Francisco, 1975).
[27] C. Weiss and N. Teichmann, Phys. Rev. Lett. **100**, 140408 (2008).
[28] B. Gertjerenken and C. Weiss, Phys. Rev. A **88**, 033608 (2013).
[29] E. M. Graefe and H. J. Korsch, Phys. Rev. A **76**, 032116 (2007).
[30] F. Nissen and J. Keeling, Phys. Rev. A **81**, 063628 (2010).
[31] M. Chuchem, K. Smith-Mannschott, M. Hiller, T. Kottos, A. Vardi, and D. Cohen, Phys. Rev. A **82**, 053617 (2010).
[32] L. Simon and W. T. Strunz, Phys. Rev. A **86**, 053625 (2012).
[33] E. M. Graefe, H. J. Korsch, and M. P. Strzys, J. Phys. A: Math. Theor. **47**, 085304 (2014).
[34] Y. Castin and R. Dum, Phys. Rev. Lett. **79**, 3553 (1997).